In situ laser-Raman imagery of Precambrian microscopic fossils

Anatoliy B. Kudryavtsev*†, J. William Schopf‡§, David G. Agresti*, and Thomas J. Wdowiak*

*Astro and Solar System Physics Program, Department of Physics, and †Center for Biophysical Sciences and Engineering, University of Alabama, Birmingham, AL 35294-1170; and ‡Department of Earth and Space Sciences, Institute of Geophysics and Planetary Physics (Center for the Study of the Evolution and Origin of Life), and Molecular Biology Institute, University of California, Los Angeles, CA 90095

Laser-Raman imagery is a sensitive, noninvasive, and nondestructive technique that can be used to correlate directly chemical composition with optically discernable morphology in ancient carbonaceous fossils. By affording means to investigate the molecular makeup of specimens ranging from megascopic to microscopic, it holds promise for providing insight into aspects of organic metamorphism and biochemical evolution, and for clarifying the nature of ancient minute fossil-like objects of putative but uncertain biogenicity.

Unlike the familiar Phanerozoic history of megascopic life, evolution during earlier and much longer Precambrian time centered on development of metabolic and biochemical capabilities in microscopic prokaryotes (1). But, because prokaryotes are highly diverse physiologically and those having similar appearances can differ markedly in metabolism and biochemistry, the sorting out of such capabilities among Precambrian fossil microorganisms requires more than traditional morphology-focused paleontology. Over recent decades, this need has been met by chemical analyses of whole rock acid-resistant carbonaceous residues (kerogens), studies that, in concert with the micropaleontologic record (2), have traced the isotopic signature of photosynthetic carbon fixation to ≈3,500 mega-annum (Ma) ago (3, 4). Measurements on bulk samples, however, cannot provide information about the composition, biochemistry, or phylogenetic relations of individual minute fossils. This deficiency has recently been offset in part by use of the ion microprobe to analyze single microfossils (5), a promising technique for determination of elemental and isotopic compositions. As reported here, laser-Raman spectroscopic imagery of individual microscopic fossils provides means by which to extend available analytical data to a molecular level. In particular, results obtained in this initial study demonstrate the applicability of this technique to analysis *in situ* of micrometer-sized organic-walled fossils, provide insight into the molecular makeup and fidelity of preservation of the carbonaceous matter of which they are composed, and show promise for clarifying the nature of ancient minute fossil-like objects of putative but uncertain biogenicity, whether in Precambrian (6, 7) or extraterrestrial materials (8).

Methods

Samples. To investigate the efficacy of the technique, kerogenous fossils three-dimensionally permineralized in cryptocrystalline chert were analyzed from three geologic units of differing metamorphic grades: axes of petrified fossil ferns from the essentially unmetamorphosed ≈45-Ma-old Clarno Formation of north-central Oregon [Precambrian Paleobiology Research Group (PPRG) sample no. 456 (9)]; tubular sheaths of oscillatoriacean cyanobacteria from silicified conical stromatolites of the subgreenschist facies ≈650-Ma-old Chichkan Formation of southern Kazakstan [PPRG sample no. 1473 (10, 11)]; and filamentous fossil microbes from silicified domical stromatolites of the greenschist facies ≈2,100-Ma-old Gunflint Formation of southern Ontario, Canada [PPRG sample no. 1289 (12, 13)].

Technique. Laser-Raman spectroscopy was performed by using a Dilor XY 0.8-m triple-stage system with macro, micro, and confocal line-scan imaging options that permit acquisition not only of individual point spectra but also of true Raman images that display the distribution of molecular components. A Coherent krypton ion laser equipped with appropriate optics provides laser wavelengths ranging from blue to infrared, of which 476, 531, 568, 647, and 752 nm were used here, typically at a laser power <15 mW over a 1-μm spot. Fossil specimens situated within the uppermost ≈30 μm or exposed at the upper surfaces of polished petrographic thin sections were centered in the path of the laser beam projected through an Olympus BX40 microscope, and a rectangular area was selected for Raman imaging. Backscattered Raman spectra obtained within each rectangle were then collected through the same optical system along micrometer-resolution scan lines, and their *x*–*y* registrations were automatically recorded to provide a pixel-assigned array of spectral elements ("spexels"). The several hundred spexels thus obtained for each specimen constitute a virtual image that was then processed into a map-like Raman image showing the areal distribution of the fossil structures that produced the Raman spectral bands originating from specific molecular components. In essence, this noninvasive, nondestructive technique can be regarded as a kind of "chemical imaging."

Results

Optical and Raman images of selected areas of fossils from the three geologic units are shown in Fig. 1, together with Raman spectra of the dominant spectral features, vibrational bands at ≈1,350 cm^{-1} and ≈1,600 cm^{-1} characteristic of carbonaceous materials, which are commonly designated "D" (disordered) and "G" (graphitic), respectively, owing to their occurrence in various forms of graphite (14). The results shown establish the carbonaceous composition of the fossils analyzed and demonstrate that the technique is applicable to specimens ranging from megascopic (Fig. 1*A*) to as small as ≈1 μm (Fig. 1*D*). Because the spatial resolution potentially attainable by the technique is limited primarily by diffraction of the excitation laser beam, it should be applicable also to submicrometer-sized structures.

As shown also in Fig. 1, the peak height of the G band relative to that of the D band increases among the specimens analyzed with increasing metamorphic grade. Thus, as in earlier studies of graphitic materials in which such relative changes in peak height were found to correlate with the extent of their structural order (14), increasing geochemical alteration produces increasingly more ordered carbonaceous matter. In comparison with the microbial Precambrian specimens (Fig. 1 *B–D*), cell walls of the much younger and essentially unmetamorphosed Eocene fern axes (Fig. 1*A*) exhibit higher luminescence relative to the Raman signal, especially at longer laser excitation wavelengths, a signature evidently reflecting the preservation of relatively less altered organic constituents.

Abbreviations: Ma, mega-annum; D, disordered; G, graphitic.

§To whom reprint requests should be addressed. E-mail: schopf@ess.ucla.edu.
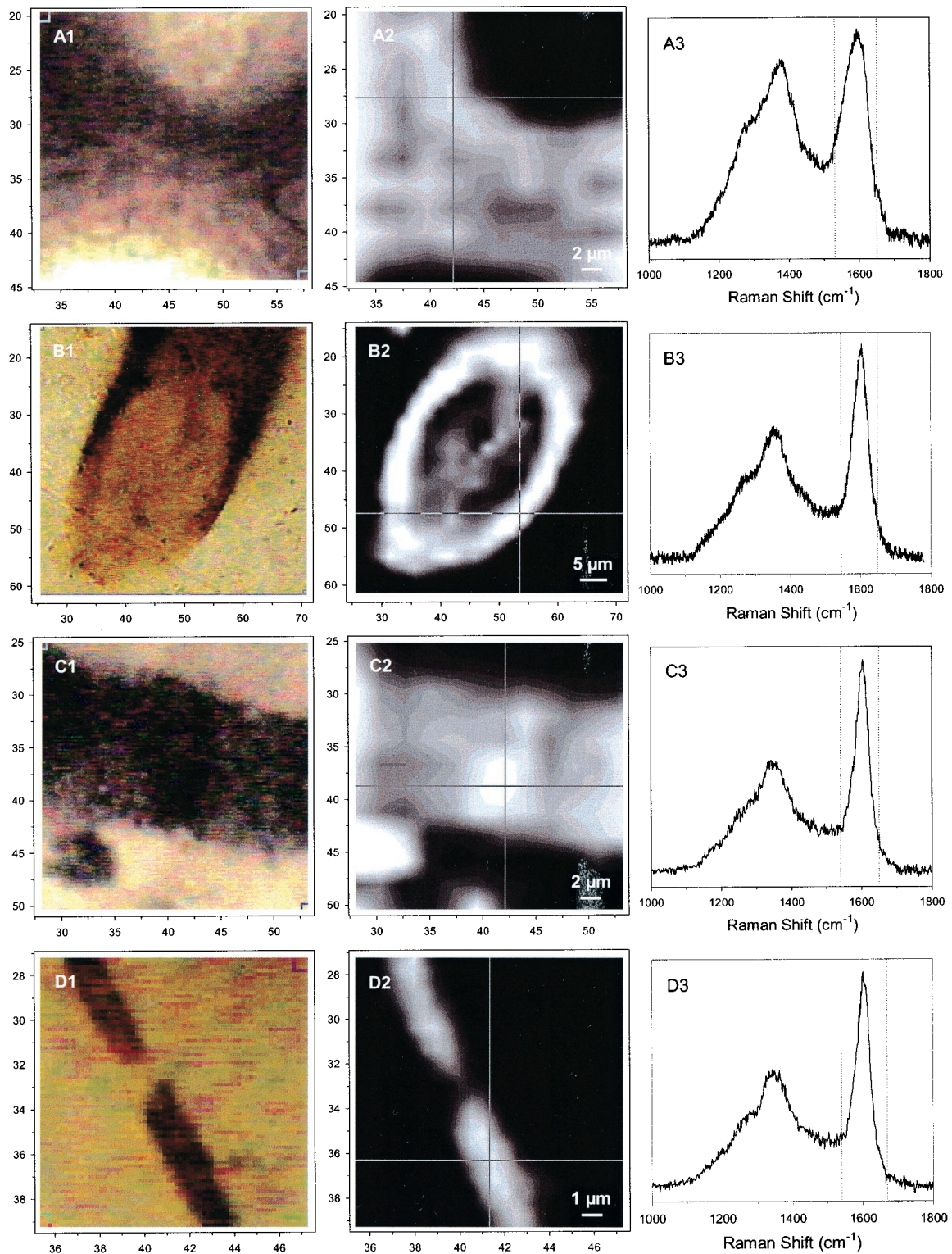
GEOLOGY

SPECIAL FEATURE

Fig. 1. Optical images (column 1), Raman images (column 2), and spectral bands used for Raman imaging (column 3) of permineralized carbonaceous fossils at or near the upper surfaces of polished chert thin sections: (*A*) Cell wall in the conductive tissue (lignified xylem) of an aquatic fern cf. *Dennstaedtia* from the essentially unmetamorphosed ≈45-Ma-old Clarno Formation of Oregon. (*B*) Tangential section of the tubular sheath of a *Lyngbya*-like oscillatoriacean cyanobacterium in a conical stromatolite (*Conophyton gaubitza*) from the subgreenschist facies ≈650-Ma-old Chichkan Formation of Kazakstan. (*C*) Transverse cell wall of a broad cellular trichome (*Gunflintia grandis*), and (*D*) a narrow prokaryotic filament (*G. minuta*), in domical stromatolites of the greenschist facies ≈2,100-Ma-old Gunflint Formation of Ontario, Canada. Each Raman image was produced by combining several hundred pixel-assigned point spectra ("spexels"), like those shown for each specimen in column 3, acquired over a small square part of the total area analyzed. The resolution of the Raman images is defined by the pixel dimensions of their component spexels; for *A*–*C*, 2 μm per pixel, and for *D*, 0.5 μm per pixel.

Four lines of evidence indicate that, rather than being derived from crystalline graphite, the two prominent bands shown in Fig. 1 actually reflect the abundant presence of aromatic organic compounds produced by geochemical alteration, principally by heating, of original biochemical components.

Presence of a Shoulder on the Low-Frequency Side of the D Band. In spectra of graphitic crystalline material, as measured by us[¶] and reported by others (16), the D band is notably symmetric. In contrast, spectra of the fossils (Fig. 1) exhibit an evident shoulder at $\approx 1,250$ cm^{-1}.

Lack of Shift of D Band Center with Laser Excitation Wavelength. In disordered graphitic materials, the position of the D band varies with excitation laser photon energy (≈ 50 cm^{-1}/eV) by means of a resonance Raman process (17, 18). Such dependence was not observed in Raman spectra of the fossils (at a detection limit of ≈ 10 cm^{-1}/eV) analyzed at the five excitation laser wavelengths that ranged from the blue (2.61 eV) to the infrared (1.65 eV).

Absence of Characteristic Second-Order Peak. Graphitic materials exhibit, in general, a prominent, well-defined, second-order band at $\approx 2,700$ cm^{-1} or about twice the D-band frequency (18), which was not observed in spectra of the fossil specimens analyzed here.

Reduction of Shoulder Intensity After Local Heating. To assess the effect of local intense heating on a geochemically relatively unaltered fossil specimen, a 1-μm portion of a cell wall, like that illustrated in Fig. 1A, was exposed to ≈ 25 times increased laser excitation power for about 5 min. As shown in Fig. 2, this experiment resulted in a significant decrease in the D band shoulder area and conversion of the spectrum to one having a decidedly more graphitic appearance.

Thus, the D band shoulder appears to be a signature of carbonaceous matter intermediate between original biological components and structurally altered products of their geochemical degradation, an interpretation consistent with recent studies (19) showing that thermal alteration of polyparaphenyl (a benzenoid composed of benzene rings linked at their para positions) to yield quinoid polymeric aromatics results in Raman spectra very similar to those observed here. It must be emphasized, however, that simple structures, such as benzenoid and quinoid polymers, should be regarded as merely representative, in a very general way, of a class of structural units that are evidently abundant in the fossils. This is because a shoulder, such as that present on the D band, is not an unambiguous indicator of a functional group of a molecular structure. Rather, this shoulder appears to be the signature of aromatic-rich fossil organic matter that is geochemically relatively well preserved, having been subjected only to low-grade metamorphic alteration (greenschist facies or below). Ongoing studies will investigate whether laser-Raman imagery can be used to detect functional groups such as C—H and N—H moieties in well-preserved carbonaceous fossils

Fig. 2. Raman point spectra acquired from a 1-μm-sized portion of a petrified cell wall of a fern axis from the Eocene Clarno Formation (*cf.* Fig. 1A) showing that intense laser heating for ≈ 5 min results in conversion of the carbon "D" band, asymmetrical because of its prominent shoulder at ≈ 1250 cm^{-1} (lower spectrum), to a more nearly symmetrical form (upper spectrum).

and, thus, the extent to which this technique can be expected to provide direct evidence of original biochemical compositions.

Conclusion

This study shows that Raman imagery can be used to correlate directly chemical composition with optically discernable morphology in ancient carbonaceous fossils. Noninvasive and nondestructive, it is a sensitive technique for measuring *in situ* the fidelity of preservation and degree of metamorphic alteration of preserved carbonaceous matter that, because of its applicability to specimens ranging in size to a small as 1 μm, can be used to analyze chemically not only morphologically intact fossils, such as petrified woods and structurally preserved microbes, but particulate kerogenous matter also. By providing insight into the molecular (carbonaceous, aromatic) makeup of the material investigated, Raman spectroscopic imagery holds promise for clarifying the nature of ancient minute fossil-like objects of putative but uncertain biogenicity, whether Precambrian or extraterrestrial (e.g., if found in meteorites or in samples brought to Earth from other planets).

[¶]For example, in $\approx 3,350 \pm 110$-Ma-old samples of Archean carbonaceous cherts of the Barberton Greenstone Belt (15) and in samples of Allende and Murchison carbonaceous chondritic meteorites.

1. Schopf, J. W. (1992) in *The Proterozoic Biosphere: A Multidisciplinary Study*, eds. Schopf, J. W. & Klein, C. (Cambridge Univ. Press, New York), pp. 587–593.
2. Schopf, J. W. (1993) *Science* **260,** 640–646.
3. Schidlowski, M., Hayes, J. M. & Kaplan, I. R. (1983) in *Earth's Earliest Biosphere: Its Origin and Evolution*, ed. Schopf, J. W. (Princeton Univ. Press, Princeton, NJ), pp. 149–186.
4. Strauss, H., Des Marais, D. J., Hayes, J. M. & Summons, R. E. (1992) in *The Proterozoic Biosphere: A Multidisciplinary Study*, eds. Schopf, J. W. & Klein, C. (Cambridge Univ. Press, New York), pp. 117–127.
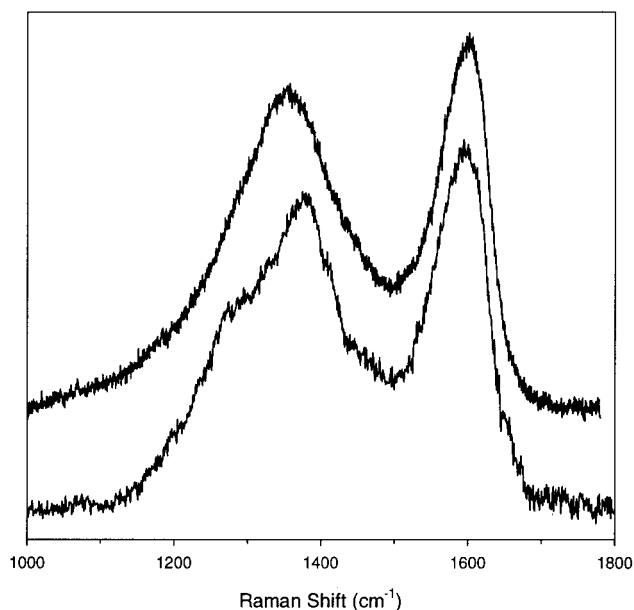5. House, C. H., Schopf, J. W., McKeegan, K. D., Coath, C. D., Harrison, T. M. & Stetter, K. O. (2000) *Geology* **28,** 707–710.
6. Schopf, J. W. & Walter, M. R. (1983) in *Earth's Earliest Biosphere: Its Origin and Evolution*, ed. Schopf, J. W. (Princeton Univ. Press, Princeton, NJ), pp. 1214–1239.
7. Mendelson, C. V. & Schopf, J. W. (1992) in *The Proterozoic Biosphere: A Multidisciplinary Study*, eds. Schopf, J. W. & Klein, C. (Cambridge Univ. Press, New York), pp. 865–951.
8. McKay, D. S., Gibson, E. K., Jr., Thomas-Keprta, K. L., Vali, H., Romanek, C. S., Clemett, S. J., Chiller, X. D. F., Maechling, C. R. & Zare, R. N. (1996) *Science* **273,** 924–930.

GEOLOGY

SPECIAL FEATURE

9. Walter, M. R., Hofmann, H. J. & Schopf, J. W. (1983) in *Earth's Earliest Biosphere: Its Origin and Evolution*, ed. Schopf, J. W. (Princeton Univ. Press, Princeton, NJ), p. 413.

10. Moore, T. B. & Schopf, J. W. (1992) in *The Proterozoic Biosphere: A Multidisciplinary Study*, eds. Schopf, J. W. & Klein, C. (Cambridge Univ. Press, New York), p. 623.

11. Schopf, J. W. & Sovietov, Y. K. (1976) *Science* **193,** 143–146.

12. Moore, T. B. & Schopf, J. W. (1992) in *The Proterozoic Biosphere: A Multidisciplinary Study*, eds. Schopf, J. W. & Klein, C. (Cambridge Univ. Press, New York), p. 679.

13. Barghoorn, E. S. & Tyler, S. A. (1965) *Science* **147,** 563–577.

14. Tuinstra, F. & Koenig, J. L. (1970) *J. Chem. Phys.* **53,** 1126–1130.

15. Wdowiak, T. J., Agresti, D. G., Mirov, S. B., Kudryavtsev, A. B., Beegle, L. W., DesMarais, D. J. & Tharpe, A. F. (1997) in *Conference on Early Mars: Geologic and Hydrologic Evolution, Physical and Chemical Environments, and the Implications for Life*, eds. Clifford, S. M., Treiman, A. H., Newsom, H. E. & Farmer, J. D. (Lunar and Planetary Institute Contribution No. 916, Houston), pp. 81–82.

16. Wopenka, B. & Pasteris, J. D. (1993) *Am. Mineralogist* **78,** 533–557.

17. Matthews, M. J., Pimenta, M. A., Dresselhaus, G., Dresselhaus, M. S. & Endo, M. (1999) *Phys. Rev. B Condens. Matter* **59,** R6585–R6588.

18. Vidano, R. P, Fischbach, D. B., Willis, L. J. & Loehr, T. M. (1981) *Solid State Commun.* **39,** 341–344.

19. Marucci, A., Pimenta, M. A., Brown, S. D. M., Matthews, M. J., Dresselhaus, M. S. & Endo, M. (1999) *J. Mater. Res.* **14,** 3447–3454.